Novel Hybridization of Parameter and Topology Optimizations: Application to Permanent Magnet Motor

Shingo Hiruma[1,2], Makoto Ohtani[3], Shingo Soma[3], Yoshihisa Kubota[3], Hajime Igarashi[1], *Member, IEEE*

[1]Graduate School of Information Science and Technology, Hokkaido University, Hokkaido 060-0814, Japan
[2]Research Fellow of Japan Society for the Promotion of Science (JSPS), Tokyo 102-0083, Japan
[3]Honda R&D Co., Ltd. Automobile R&D Center, Tochigi 321-3393, Japan

This paper introduces novel hybridization of parameter optimization (PO) and topology optimization (TO) methods. The proposed method is applied to the optimization of a permanent magnet motor. The magnet shape and topology of the flux barrier of the rotor core are optimized by performing PO and TO simultaneously. In the optimization, automatic mesh generation is adopted to improve the resolution of the shape representation. It is shown that the increase in the average torque resulting from the proposed hybrid optimization is larger than that obtained by the conventional TO in which only the topology of the flux barrier is optimized. The decomposition of the total torque to the magnet and reluctance torques suggests that the reluctance torque is effectively generated in the rotor optimized by the proposed method.

***Index Terms*— Automatic mesh generation, genetic algorithm, parameter optimization, permanent magnet motors, topology optimization.**

I. Introduction

Shape optimization is an important technique for improving the efficiency of permanent magnet (PM) motors. Shape optimization conventionally uses either parameter optimization (PO) or topology optimization (TO) method. PO is useful when optimizing user-defined design variables such as size, position, angle, and number of parts. The advantage of PO lies in the fact that the shape of a material, for example, PM, can be parameterized considering the actual possibility in manufacturing. TO [1]–[5] is useful when it is difficult to parameterize the shape or assume the topology as in the case of flux barriers. Because of the nature of TO, it can lead to a novel design that has never been reported.

In this paper, we propose a new optimization method that combines the PO and TO methods. Although the proposed method is general, we restrict ourselves to the design of PM motors. We apply PO to the design of PMs to make the shape meet the manufacturing constraints, whereas we adopt TO to design the flux barrier. In TO, the normalized Gaussian network (NGnet) is used to represent the material distribution. This means that the material distribution is parameterized by the weights of the NGnet. Owing to this property, the problem is reduced to a PO problem, which is solved by the genetic algorithm (GA) with a global search. It might be difficult to apply this parametrization approach to gradient-based methods such as the level set method and density method.

The proposed hybrid optimization method is applied to the multi-objective optimization problem of an interior permanent magnet (IPM) motor where the average torque is maximized while the torque ripple is minimized. The proposed method was compared with the conventional TO method. Moreover, the IPM motors with the U- and V-shaped magnets are optimized using the proposed method to verify its feasibility.

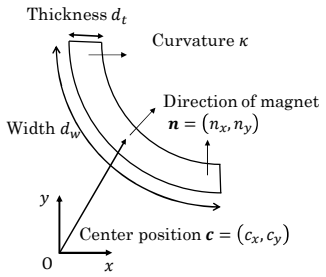

Fig. 1. Parametrization of PM

II. Hybrid Optimization Method

A. Parameter optimization

PO is widely performed in industries to optimize user-defined design variables, such as size, position, angle, and number of parts. For example, let us consider the shape optimization of a magnet in an IPM motor, which is represented by five parameters: width d_w, thickness d_t, curvature κ, direction of the magnet $\boldsymbol{n} = (n_x, n_y)$, and center position $\boldsymbol{c} = (c_x, c_y)$ as shown in Fig. 1. In numerous cases, there would be restrictions in the magnet shape due to the constraints arising from volume, manufacturing, and cost. Using the parameter representation, we can readily introduce these constraints to the optimization. Therefore, PO has this advantage for the optimization of magnet shape in comparison with TO.

B. Topology optimization

In contrast to the shape optimization of magnets, we encounter situations where it is difficult to define the design

Manuscript received April 1, 2015; revised May 15, 2015 and June 1, 2015; accepted July 1, 2015. Date of publication July 10, 2015; date of current version July 31, 2015. (Dates will be inserted by IEEE; "published" is the date the accepted preprint is posted on IEEE Xplore®; "current version" is the date the typeset version is posted on Xplore®). Corresponding author: S. Hiruma (e-mail: hiruma@em.ist.hokudai.ac.jp).

Color versions of one or more of the figures in this paper are available online at http://ieeexplore.ieee.org.

Digital Object Identifier (inserted by IEEE).

variables for the shape or assume the topology as in the case of the flux barriers in the IPM motors. The shape optimization of the flux barriers requires topological changes such as generation and annihilation of holes and free deformation of material boundaries. For this purpose, TO should be employed because of its flexibility in shape representation. In TO, there are several methods for representing and evolving the topology, for example the gradient method using level set function [1], [2], density method [3], and metaheuristic method based on the NGnet on/off method [4], [5]. In this study, we employ the metaheuristic method based on the NGnet method because it is compatible with PO.

In the NGnet method, the material distribution is represented by the zero-valued contour of the NGnet $\varphi(\boldsymbol{x}, \boldsymbol{w})$ which is given by

$$\varphi(\boldsymbol{x}, \boldsymbol{w}) = \sum_{i=1}^{n_{\mathrm{ng}}} w_i b_i(\boldsymbol{x}) \tag{1a}$$

$$b_i(\boldsymbol{x}) = \frac{G(\boldsymbol{x}; \boldsymbol{\mu}_i, \Sigma)}{\sum_{j=1}^{n_{\mathrm{ng}}} G(\boldsymbol{x}; \boldsymbol{\mu}_j, \Sigma)} \tag{1b}$$

$$G(\boldsymbol{x}; \boldsymbol{\mu}_i, \Sigma) = \exp\left(-\frac{1}{2}(\boldsymbol{x} - \boldsymbol{\mu}_i)^{\mathrm{T}} \Sigma^{-1} (\boldsymbol{x} - \boldsymbol{\mu}_i)\right) \tag{1c}$$

where $\boldsymbol{x}, \boldsymbol{w}, b_i$ and n_{ng} denote the position in the Cartesian coordinate system $\mathbb{R}^d$, weighting vector in $\mathbb{R}^{n_{\mathrm{ng}}}$ composed of $w_i, i = 1,2, \dots, n_{\mathrm{ng}}$, the i-th normalized Gaussian function and their number, respectively. The Gaussian $G(\boldsymbol{x}; \boldsymbol{\mu}_i, \Sigma)$ is parameterized by the centroid $\boldsymbol{\mu}_i \in \mathbb{R}^d$ and covariance matrix $\Sigma \in \mathbb{R}^{d \times d}$ which are defined *a priori* in the design region. Because we consider the two-dimensional optimization problem in this paper, d is set to 2, and $\Sigma = \mathrm{diag}[\sigma^2, \sigma^2]$. The Gaussians are arranged with mutual distance of the standard deviation σ. The NGnet $\varphi(\boldsymbol{x}, \boldsymbol{w})$ is defined by the linear combination of the normalized Gaussians, which is expected to represent arbitrary functions if n_{ng} is sufficiently large. The distribution of the material attribute $A(\boldsymbol{x}, \boldsymbol{w}) = \{\mathrm{iron}, \mathrm{air}\}$ is determined from

$$A(\boldsymbol{x}, \boldsymbol{w}) = \begin{cases} \text{magnetic steel} & \text{if } \varphi(\boldsymbol{x}, \boldsymbol{w}) \geq 0 \\ \text{air} & else \end{cases}. \tag{2}$$

The material distribution $A(\boldsymbol{x}, \boldsymbol{w})$ is dependent on the weights $\boldsymbol{w}$, which are chosen as the design variables for the NGnet-based TO. Notably, the material distribution is parameterized by $\boldsymbol{w}$ that has n_{ng} degree of freedoms. Owing to this property of the NGnet method, we can reduce our problem to a PO problem with respect to $\boldsymbol{w}$ and the magnet-shape parameters, of which the gene is composed in GA with global search.

C. *Improving resolution of shape representation*

In the previous studies on NGnet-based TO [5], the distribution of the material attribute $A(\boldsymbol{x}, \boldsymbol{w})$ was evaluated for each element in a fixed finite element mesh. This method is called the on/off method, and it does not require mesh generation. However, it produces jagged shapes that are not favorable for manufacturing. Although we can improve the resolution of the shape representation by increasing the number of finite elements, it increases the computational time of the finite element analysis (FEA). To avoid this problem, we perform mesh generation for the new magnet configuration. The mesh generation is performed by an open source software (https://github.com/MmgTools/mmg) that implements the 'implicit domain meshing' proposed in [6]. In the implicit domain meshing, we input a base mesh and values of a 'level set' function on its vertices, and we obtain a new mesh that has material boundaries corresponding to the zero-valued contour of the input level set function, as shown in Fig. 2. The values of the shape function $\varphi(\boldsymbol{x}, \boldsymbol{w})$ are input as a level set function. In the optimization, we also create shape function $s(\boldsymbol{x}, \boldsymbol{p})$ which expresses the shape of the magnet by the zero-valued contour and generates a new mesh that contains magnets. The average time to perform the mesh generation is approximately a few seconds, which is much shorter than that for performing FEA for magnetostatic analysis. This approach also reduces the computing time for the optimization because we have to make fine discretization to avoid the jagged shapes when we use the fixed mesh.

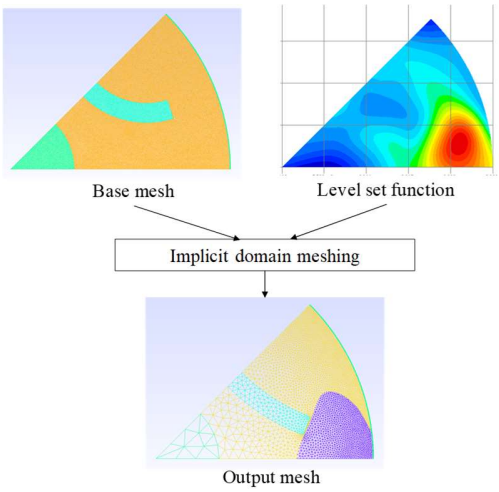

Fig. 2. Flow of implicit domain meshing

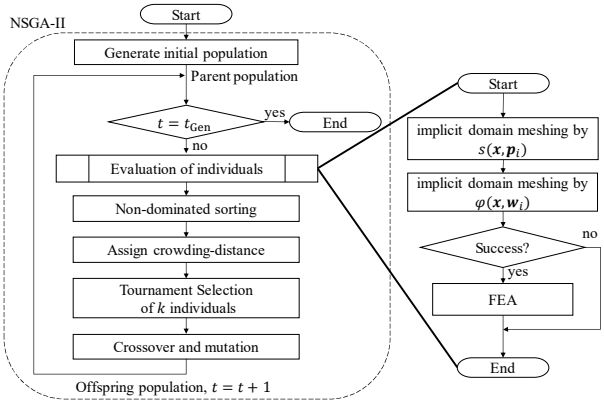

Fig. 3 Flow diagram of proposed optimization using NSGA-II

D. *Optimization flow diagram*

Let $\boldsymbol{p}, \boldsymbol{w}$ be the magnet-shape parameters and weights of the NGnet, respectively. We can express the optimization problem

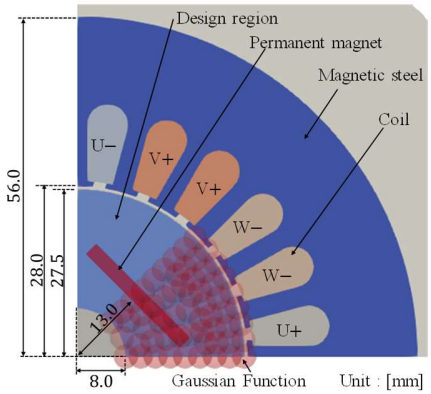

Fig. 4. IPM motor. Red circles represent the Gaussian functions

TABLE I
PARAMETERS FOR FEA* AND NSGA-II

Number of genes	60 ,61
Number of population	360
Number of individuals k	120
Number of generations	700
Speed [rpm]	1800
Current phase angle [degree]	20
Current amplitude [A]	3.0
Number of poles	4
Number of turns	35
Residual flux density [T]	1.4
Magnetic steel sheet	50A400
Thickness [mm]	65

*In-house software is used for FEA

as follows:

$$\text{maximize } f_i(\boldsymbol{p},\boldsymbol{w}), \text{sub. to } g_i(\boldsymbol{p},\boldsymbol{w}) \geq 0, i = 1,2,\ldots. \quad (3)$$

This problem is solved by the GA. To treat the multi-objective function, we employ non-dominated sorting genetic algorithms (NSGA) -II [7]. The optimization flow diagram of the proposed method is shown in Fig. 3. The individual j has the data $\boldsymbol{p}_j, \boldsymbol{w}_j$ and the mesh generation is performed by the implicit domain meshing before FEA. However, the mesh generation sometimes fails due to unrealizable material distribution, for example a very thin magnetic-core region. Also, we sometimes have unacceptably flat finite elements. In these cases, we do not perform FEA for the individual and neglect it by setting a death penalty on the objective functions $f_i(\boldsymbol{p}_j,\boldsymbol{w}_j), i = 1,2,\ldots.$

III. Optimization Results

A. Comparison with conventional motors

We consider the hybrid optimization of the rotor of the IPM motor shown in Fig. 4, in which 60 Gaussian functions, and $\sigma = 0.002$, are uniformly deployed. In this problem, the magnet curvature $0 < p_1 = \kappa \leq 100$ and flux barriers are optimized (Model P1). For comparison, we perform the conventional TO of the flux barriers in the rotor that includes a fixed plane magnet. The optimization problem is defined by

$$\text{maximize } f_1(\boldsymbol{p},\boldsymbol{w}) = T_{\text{avg}} - (n_{\text{connect}} - 1) \quad (4a)$$
$$\text{minimize } f_2(\boldsymbol{p},\boldsymbol{w}) = T_{\text{max}} - T_{\text{min}} + (n_{\text{connect}} - 1) \quad (4b)$$

where T_{avg} is the average torque, T_{max}, and T_{min} are the maximum and minimum torque values, respectively, and n_{connect} denotes the number of connected magnetic cores. The second term of both equations in (4) is introduced to avoid separation of the magnetic core. The settings for the optimization and FEA are summarized in Table I. Note that the number of the genes is 60, and 61 in the conventional TO, hybrid optimization, respectively.

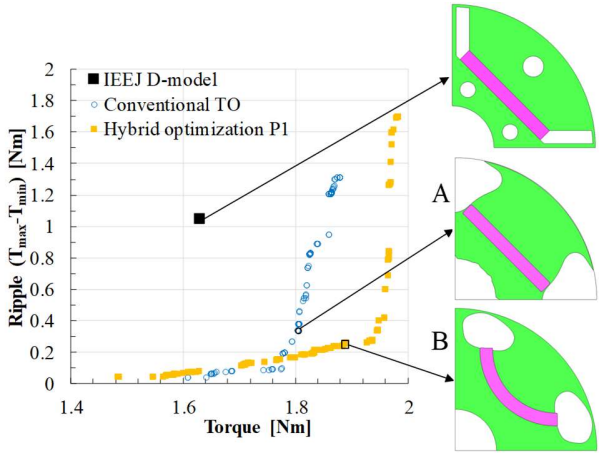

Fig. 5. Pareto-fronts obtained by the conventional TO and hybrid optimization, and typical rotors A, B.

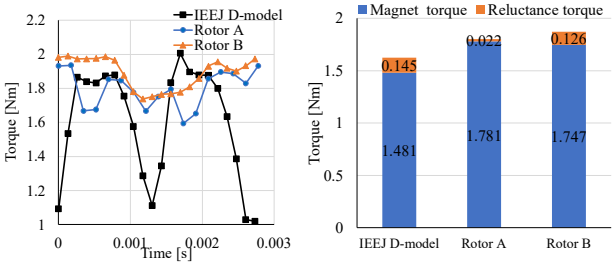

Fig. 6. Time variation of torque (left) and average torque decomposition (right) of rotors A, B.

TABLE II
MAGNET FLUX AND DQ INDUCTANCES OF IEEJ D-MODEL, ROTORS A, B

	Φ_a [Wb]	L_d [H]	L_q [H]
IEEJ D-model	2.14×10^{-1}	1.01×10^{-2}	2.68×10^{-2}
Rotor A	2.58×10^{-1}	7.42×10^{-3}	9.95×10^{-3}
Rotor B	2.53×10^{-1}	6.93×10^{-3}	2.15×10^{-2}

The resultant Pareto fronts and typical rotors, marked by A, and B, are shown in Fig. 5. Rotors A and B are obtained by the conventional TO and proposed hybrid optimization, respectively. Numerous solutions on the Pareto front which have larger average torque are found to have a thin magnetic core between the air gap and flux barrier. Rotor B has a relatively thick magnetic core. The time variation of torque and decomposition of the average torque into the magnet T_{mag} and the reluctance T_{rel} torques are plotted in Fig. 6. The two components are computed by

$$T_{\text{mag}} = p\Phi_{\text{a}} i_{\text{q}} \quad (5a)$$
$$T_{\text{rel}} = p\left(L_{\text{d}} - L_{\text{q}}\right) i_{\text{d}} i_{\text{q}} \quad (5b)$$

where $p, \Phi_{\text{a}}, L_{\text{d}}, L_{\text{q}}, i_{\text{d}}, i_{\text{q}}$ are the number of the pole pairs, magnet flux, d-axis inductance, q-axis inductance, d-axis current, and q-axis current, respectively [8]. The values of $\Phi_{\text{a}}, L_{\text{d}}, L_{\text{q}}$ are summarized in TABLE II. The average torques of Rotors A and B are 1.80 and 1.87 Nm, and the ripples are 0.34

and 0.25 Nm, while the normalized ripples are 19% and 13%, respectively.

The decomposition of the total torque suggests that Rotor A maximizes the magnet torque T_{mag} while Rotor B maximizes the total torque by increasing the reluctance torque T_{rel}. As can be seen from TABLE II, Rotor B increases the q-axis inductance, which makes it possible to increase the total torque. These trends can also be found in the populations in the Pareto front obtained by TO and the hybrid optimization.

B. Optimization of rotor with U-shaped and V-shaped magnets

We optimize the curvature p_1 and distance p_2 from the origin of the U-shaped magnet (Model P2) shown in Fig. 7. Moreover, we also consider a V-shaped magnet for which we change the distance p_1 from the origin and direction of the magnets represented by p_2, p_3 (Model P3). The number of parameters is 2 in P2 and 3 in P3. The resultant Pareto fronts and typical Rotors B to D are shown in Fig. 8. The Pareto front for Model P1 and Rotor B are the same as those in Fig. 5. The average torque and ripple of Rotors B to D are summarized in TABLE III. We also provide the information about the minimum thickness of the magnetic core d_{min} between the air gap and flux barrier to consider the feasibility of the optimized rotors. If one has a small value of d_{min}, there would be difficulties in manufacturing. Considering the resultant values of d_{min}, Rotors B and D would be suitable for manufacturing. Although Rotor C has a larger average torque than Rotors B and D, the thickness of C must be increased to meet the manufacturing condition.

As in the case of Rotor B, Rotor D also utilizes reluctance torque to increase the total torque. Rotor D has a V-shaped magnet, which is widely used [9].

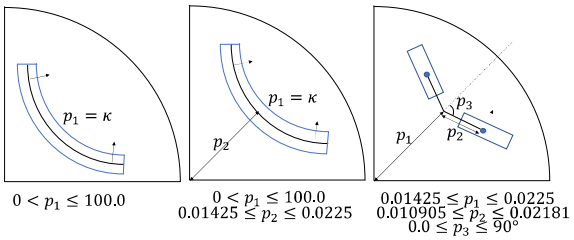

Fig. 7. Parameter settings for Models P1 (left), P2 (center), P3 (right).

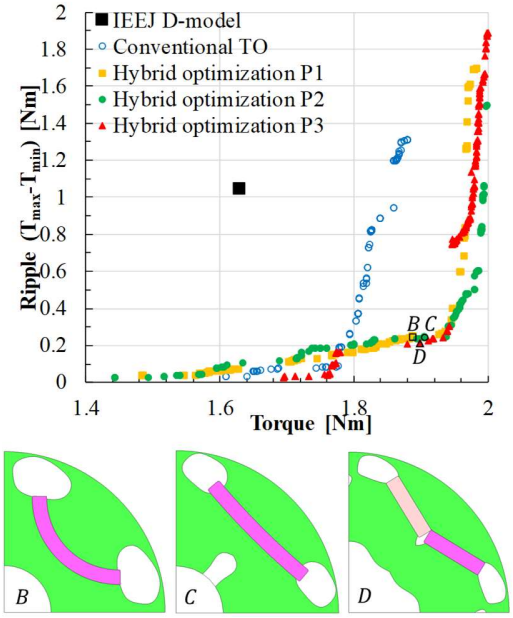

Fig. 8. Pareto-fronts (upper) and typical rotors (lower).

TABLE III
VALUES OF AVERAGE TORQUE, RIPPLE, d_{MIN} OF ROTORS B, C, AND D.

	T_{ave} [Nm]	ripple [Nm]	d_{min} [mm]
Rotor B	1.874	0.251	0.366
Rotor C	1.904	0.251	0.155
Rotor D	1.899	0.216	0.308

IV. CONCLUSION

In this paper, we proposed novel hybridization of the parameter and topology optimizations. We applied the proposed method to the optimization problem where the shape of the magnet and topology of the flux barriers are optimized simultaneously. Owing to the proposed method, we have optimized motors with different configurations of the magnet and flux barrier to achieve an appropriate balance between the average torque and ripple.

ACKNOWLEDGMENT

This work was supported in part by Grants-in-Aid for Scientific Research (KAKENHI) through the Japan Society for the Promotion of Science (JSPS) under Grant Numbers JP19J20541 and 18K18840.

REFERENCES

[1] J. Lee and S. Wang, "Topological Shape Optimization of Permanent Magnet in Voice Coil Motor Using Level Set Method," *IEEE Trans. Magn.*, vol. 48, no. 2, pp. 931–934, Feb. 2012, doi: 10.1109/TMAG.2011.2173922.

[2] Y. Yamashita and Y. Okamoto, "Design Optimization of Synchronous Reluctance Motor for Reducing Iron Loss and Improving Torque Characteristics Using Topology Optimization Based on the Level-Set Method," *IEEE Trans. Magn.*, vol. 56, no. 3, Mar. 2020, doi: 10.1109/TMAG.2019.2954468.

[3] F. Guo and I. P. Brown, "Simultaneous Magnetic and Structural Topology Optimization of Synchronous Reluctance Machine Rotors," *IEEE Trans. Magn.*, vol. 56, no. 10, Oct. 2020, doi: 10.1109/TMAG.2020.3014289.

[4] H. Sasaki and H. Igarashi, "Topology optimization using basis functions for improvement of rotating machine performances," *IEEE Trans. Magn.*, vol. 54, no. 3, Mar. 2018, doi: 10.1109/TMAG.2017.2759784.

[5] T. Sato, K. Watanabe, and H. Igarashi, "Multimaterial topology optimization of electric machines based on normalized Gaussian network," *IEEE Trans. Magn.*, vol. 51, no. 3, pp. 1–4, Mar. 2015, doi: 10.1109/TMAG.2014.2359972.

[6] C. Dapogny, C. Dobrzynski, and P. Frey, "Three-dimensional adaptive domain remeshing, implicit domain meshing, and applications to free and moving boundary problems," *J. Comput. Phys.*, vol. 262, pp. 358–378, Apr. 2014, doi: 10.1016/j.jcp.2014.01.005.

[7] K. Deb, A. Pratap, S. Agarwal, and T. Meyarivan, "A Fast and Elitist Multiobjective Genetic Algorithm: NSGA-II," *IEEE Trans. Evol. Comput.*, vol. 6, no. 2, 2002.

[8] K. Yamazaki and M. Kumagai, "Torque analysis of interior permanent-magnet synchronous motors by considering cross-magnetization: Variation in torque components with permanent-magnet configurations," *IEEE Trans. Ind. Electron.*, vol. 61, no. 7, pp. 3192–3201, 2014, doi: 10.1109/TIE.2013.2278508.

[9] A. Wang, Y. Jia, and W. L. Soong, "Comparison of five topologies for an interior permanent-magnet machine for a hybrid electric vehicle," *IEEE Trans. Magn.*, vol. 47, no. 10, pp. 3606–3609, Oct. 2011, doi: 10.1109/TMAG.2011.2157097.